AMM36
The Second TSME International Conference on Mechanical Engineering
19-21 October, 2011, Krabi

Effect of Projectile Geometry on Impact Response and Regime Characterisation

Attharat Wimonjariyaboon, Paul.W.Bland* and Sarin Tiranasawasdi

Department of Mechanical Engineering Simulation & Design,
The Sirindhorn International Thai-German Graduate School of Engineering,
King Mongkut's University of Technology North Bangkok, Bangkok 10800, Thailand.
* Corresponding Author: Tel: +66 (0) 2913 2500 ext. 2915, Fax: +66 (0) 2913 2500 ext. 2922,
E-mail: bland.p.mesd@tggs-bangkok.org

Abstract

Previous studies on the response of a flat plate to impact from a free flying projectile have identified response regimes, with boundaries and transitions defined by projectile mass and velocity, and broadly characterised as ranging from quasi-static to highly transient and localised responses. The objective of this work was to investigate the effect of projectile geometry, specifically the shaft length of a circular cross sectioned projectile with a hemispherical nose, on generating atypical responses that did not fit the regime boundary locations identified in the earlier work. Simulations with LS-DYNA included a damage mechanics model using element deletion based on reaching a critical strain, allowing for the case of perforation and continued contact forces between the projectile shaft and target during perforation. Cases with three different critical failure strains used in the damage mechanics model, as well as varying the projectile shaft length were considered, for a range of initial impact regime conditions determined by projectile mass and velocity.

For a given initial impact condition, defined by projectile velocity and mass, the type of response of the plate is strongly affected by shaft length if perforation occurs, and the longer the shaft, the greater the shift of the response from a highly transient and localised response to a quasi-static type of response. In the case of rebound, the shaft length has negligible effect on the type of plate response. This is further confirmed by observing the time evolution development of stress waves and stress profiles across the plate span, including the timing of the stress profile switching between a characteristic highly transient response type profile to a profile typical of a quasi static response. All three critical failure strain values gave the same qualitative results, with the middle value being considered to be the most realistic.

Keywords*:* Impact regimes, response, stress profiles

1. Introduction

The effect on target response and damage by changing projectile nose tip geometry [1-3] or changing angle of impact [1], have been studied, but not specifically projectile shaft length. The study of impact regimes by using stress waves was introduced in the authors' previous papers [4-6]. The regimes referred to high (H) or

low (L) projectile mass (M) and velocity (V). Extreme conditions of LV/HM showed Quasi-Static (QS) type behaviour with long contact times, continuous contact and global deflection approximated by the 1st mode response of the projectile and target as a lumped spring mass system. Extreme conditions of HV/LM showed continuous contact, short contact times and localised deflection. Between the extremes, the transitions showed discontinuous contact (multiple contacts) and a delay in the formation of a global deflection. Simulations showed that the stress profile shape of extreme HV/LM regimes changed throughout the contact duration with three identifiable phases. Extreme LV/HM stress profiles also showed a changing shape, but crucially only for the first 2-7% of the contact duration, and then switched to being a constant shape except for a scaled increased in amplitude. For impact conditions between the extremes, the switching time occurred later during contact, when moving from LV/HM to HV/LM [5].

This "switch" is a useful feature to look for in all impact events, and referred to in this paper. The switching time indicates when the stress profile changes form a typical HV/LM to typical LV/HM shape and time wise development of that shape. It is given either as an absolute measure of time, starting from the time of first contact, or as a % of the total contact time. The measurement of contact time starts when the projectile first makes contact with the target. The contact time ends when the projectile losses contact for the last time. Note, that in some conditions, projectile can make and lose contact more than once.

2. Methodology

This paper studied the effect of projectile shaft length on the type and timing of response observed during contact. Impact conditions in the extreme HV/LM regime, near and across the boundary transitions were simulated, comparing results from different projectile shaft lengths by observing the characteristic response, total contact time, the time evolution of stress profiles (normal stress and Von-Mises stress) along the span, and the switching time of stress profiles from a typical HV/LM to typical LV/HM profile. A damage model is incorporated specifically to allow for a more realistic behaviour for the case of perforation. This study used LS-DYNA, eight node, first order 3D solid elements, and due to symmetry, a quarter model to reduce computation effort. The *x* axis was defined along the span, *y* axis through the thickness, and *z* axis is across the plate width, with the origin at the centre of the plate of the top surface. The projectile basic shape was a steel cylinder with a hemispherical nose of diameter 3.94*mm* with various cylinder shaft lengths, giving projectiles of mass 1*g* with 9.18*mm* length (*L1*), 7*g* with 72.1*mm* length (*L2*), and 13*g* with 135.02*mm* length (*L3*), referred to as projectile numbers 1 to 3 respectively. Two further projectiles were used, by adding a smaller diameter cylinder to the back of the 1*g* projectile, and removing mass from the 13*g* projectile such that their masses were now 7*g*, as shown in Fig.1, but still maintaining the cylinder diameter that would be in contact with the target at 3.94*mm*. These are referred to as projectile numbers 4 and 5 respectively.

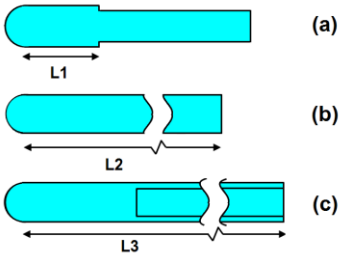

Figure 1. Projectile numbers 4, 2 & 5; (a) 1*g* projectile modified to 7*g*. (b) original 7g projectile. (c) 13*g* projectile modified to 7*g*. Shown schematically and in cross section.

Projectile velocities were 50, 70, 125, and 180*m/s* for creating different impact events such as rebounding without damage, rebounding with penetration, and full perforation. The projectile material was steel with density of 7.85E3kg/m^3. It was modelled as being rigid, partly to reduce computation time, but also as a reasonable assumption, compared to the target material. However, within LS-DYNA, it was still required to input additional properties, of Young's Modulus of 200*GPa*, and Poisson's ratio of 0.3.

The aluminium flat plates were 2*mm* thick, 150*mm* span and 80*mm* wide, rigidly clamped on their short sides. The model used isotropic kinematic hardening material with density of 2.77E3kg/m^3, Young's Modulus of 71*GPa*, Poisson's ratio of 0.33, yield strength of 280*MPa*, and tangent modulus of 500*MPa*. The strain rate was accounted for using the Cowper Symond model [7,8]. The Cowper Symond parameters *C* and *P* for aluminium were 6500 and 4, respectively. The contact model used an element erosion approach selecting the LS-DYNA "eroding nodes to surface" algorithm for the contact condition between the projectile and target. The friction coefficient between projectile and plate was 0.61 for static and 0.47 for dynamic cases [9]. An element was removed when the effective plastic strain in the element reached the critical value. This study used three values of criteria failure strain (FS) as 0.2 [7,10,11], 0.5, and 1 [8], comparing the results for each. Simulations were also run without the damage model to compare the impact response to the characteristic definitions of previous work [5,6] and also compare to the results from simulations with the damage model.

All results from simulation cases were normalized. All stresses (*Sx, Sy*, and *Sz*) were normalized with the maximum value of Von-Mises Stress (*Seqv*). Time was normalized with total contact time. The *x* direction was normalized with the span, and *y* direction normalized with plate thickness.

3. Results and Discussion

The results from the simulations without the damage model are summarised in Table 1.

Table 1. Summary initial impact response regime without damage.

Case No.	Mass (g)	Velocities (m/s)	Mass Boundary(C/D/C)							Velocity Boundary(G/D/L)						
			EL	LB	TLB	T	THB	HB	EH	EL	LB	TLB	T	THB	HB	EH
			C	C	D	D	D	C	C	G	G	D	D	D	L	L
1	1	50	■													■
2	1	70	■													■
3	1	125	■													■
4	1	180	■													■
5	7	50		■											■	
6	7	70		■											■	
7	7	125		■											■	
8	7	180				■								■		
9	13	50				■						■				
10	13	70				■							■			
11	13	125				■							■			
12	13	180				■							■			

These are the benchmark results, showing the location of the impact condition on a relative scale for the mass and velocity regime boundaries. The regimes are divided into seven ranges of extremely low (EL), low boundary of

transition (LB), in the transition but just above the low boundary (TLB), in the middle of the transition (T), in the transition but just below the high boundary (THB), high boundary of transition (HB), and extremely high (EH); applied to both mass and velocity. “C” and “D” refer to continuous and discontinuous contact respectively. “G”, “D” and “L” refer to global, delayed global and local deflection respectively.

The following sections give the main results from this work, for all simulations that included the damage model.

3.1 Effect of changing length and mass

Using projectile numbers 1 to 3 changed both the projectile shaft length and mass. Fig.2 shows the comparison of contact times of different shaft lengths and projectile masses using different critical failure strains (FS) in the damage model. “RE”, “PN” and “PF” indicate rebound with no damage, rebound with damage (partial penetration through the thickness) and perforation (full penetration through the thickness).

All cases using the 1*g* projectile (projectile number 1) resulted in RB except for two cases where FS=0.2, with PN at 125*m/s* and PF at 180*m/s*. The RB contact times for different FS but for the same velocity are all similar. A low FS is more likely to result in elements being deleted for lower strain conditions, hence at higher velocities, we start to see PN and PF.

The contact times for the 7 and 13*g* projectiles (projectiles numbers 2 and 3) were all longer compared to the 1*g* projectile. For the case of PF, this is understandable as the shaft length is much longer and must pass through the target thickness. In the case of RB or PN, the shaft length is not in contact with the target, and so this effect must only be due to the change of mass. It would also be expected that projectile number 3 with the longest shaft length, has longer contact times compared to projectile number 2. This is mostly the case except for 70*m/s* with FS=0.2, 125*m/s* with FS=0.5, and 180*m/s* with FS=1 as shown in Fig.2(a)-(c).

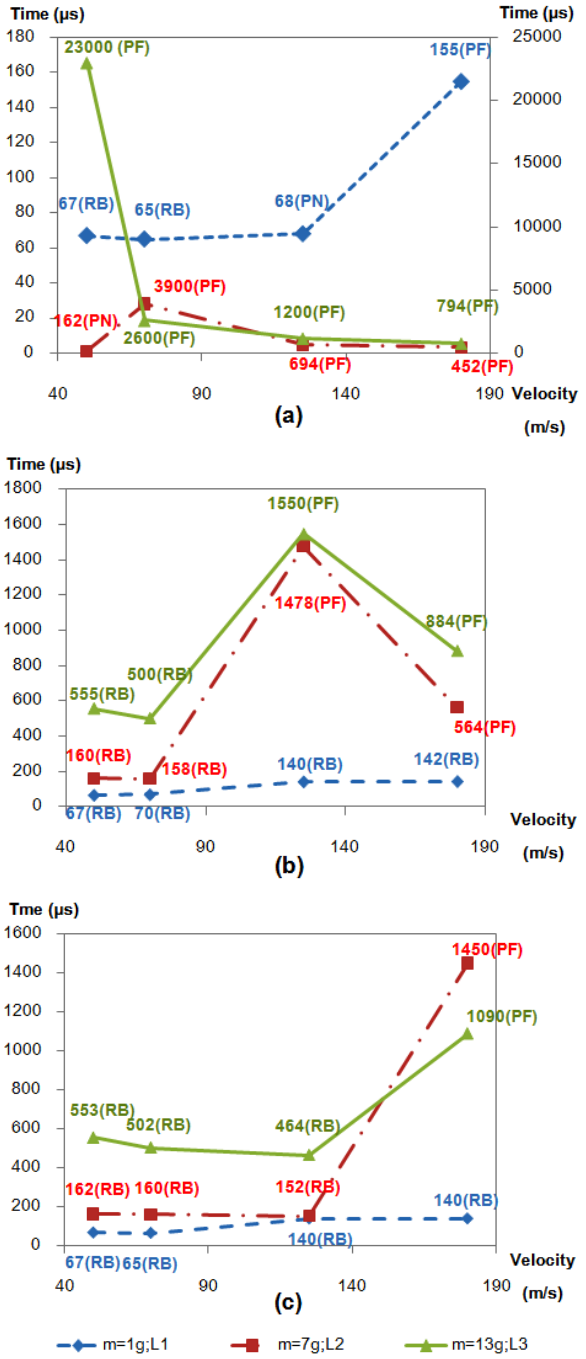

Figure 2. Comparison of total contact time for different masses, shaft lengths, velocities, and

critical failure strains: (a) FS=0.2 (b) FS=0.5 (c) FS=1.

This can be explained by considering that when increasing the impact energy, and changing from RB or PN to PF, the contact time increases significantly when there is just enough energy for PF, leaving a low projectile exit velocity. For further increases in energy, it would be expected that the contact time reduces due to the exit velocity being much higher [3]. The required impact energy to achieve the ballistic limit of PF with negligible exit velocity, is achieved at different impact velocities for these two projectiles because they have different masses. The two cases where the 7*g* projectile has a higher contact time than the 13*g* projectile correspond to having just reached the ballistic limit, but the 13*g* projectile having already passed the ballistic limit and having a significant exit velocity. This is confirmed by checking the relative exit velocities of these cases within the simulation.

A key indicator to locate the impact condition using mass and velocity scales, as described in the introduction, is the switching time. Fig.3 shows the switching times corresponding to the same simulation cases presented in Fig.2.

Note that for most 1g cases, there was no switching time as the whole impact event fell within the HV/LM regime during all contact, except for FS=0.2 at 180*m/s*. For a given FS and for different velocities but still all resulting in RB or PN, the switching % and absolute times are fairly constant. When the velocity is further increased, resulting in PF, the switching % times reduce but with some fluctuation in the absolute times that do not show a strong correlation of behaviour that can be conclude in this paper. For a given FS and a given velocity, the longer shaft and higher mass projectiles have a lower switching % time (again, the absolute switching time values show no strong correlation of behaviour) for RB, PN and PF, which indicates their impact condition is closer to the LV/HM regime boundaries or transitions.

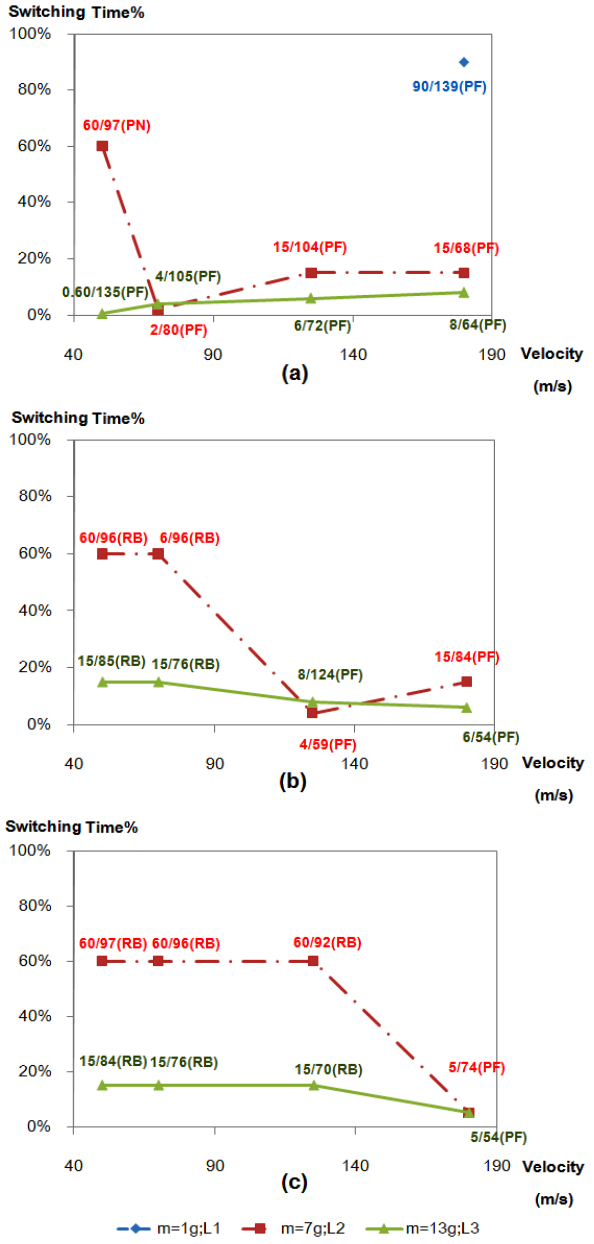

Figure 3. Comparison of switching time for different masses, shaft lengths, velocities, and critical failure strains: (a) FS=0.2 (b) FS=0.5 (c)

FS=1. Showing %/absolute values in microseconds.

For RB and PN cases, the shaft length does not play a role because the shaft is never in contact with the target, and so this effect must be only due to changing mass.

3.2 Effect of changing length only

The above results included the effect of changing mass as well as shaft length. Additional simulations using the same analysis methods were performed using projectiles numbers 2, 4 & 5, all being 7*g* but different shaft lengths. Fig.4. shows the contact times, and follows the same general trends as described in section 3.1, but now, PF occurs at the same velocity for a given FS. This clearly shows that the contact times are increased by having a longer shaft length, and reach a peak at velocities near the ballistic limit.

The velocity corresponding to the ballistic limit increases for higher FS, as more energy is required to achieve the higher required critical strains. Similarly, the trends for switching time, as shown in Fig.5., are also generally the same as described in section 3.1, with longer shaft lengths having lower switching % times.

As before, the absolute values of switching time do not show any conclusive correlation of behaviour. A key difference is removing the effect of a changing mass, resulting in the same switching % and absolute times for RB and PN cases, except FS=0.2, at the lowest velocity. This anomaly occurs because the event is near the ballistic limit, where exit velocities are very small.

The reduction of switching time from near 100% to 5-15% represents a large shift in the impact condition and response, from the HV/LM extreme regime boundary, almost completely towards the extreme LV/HM boundary.

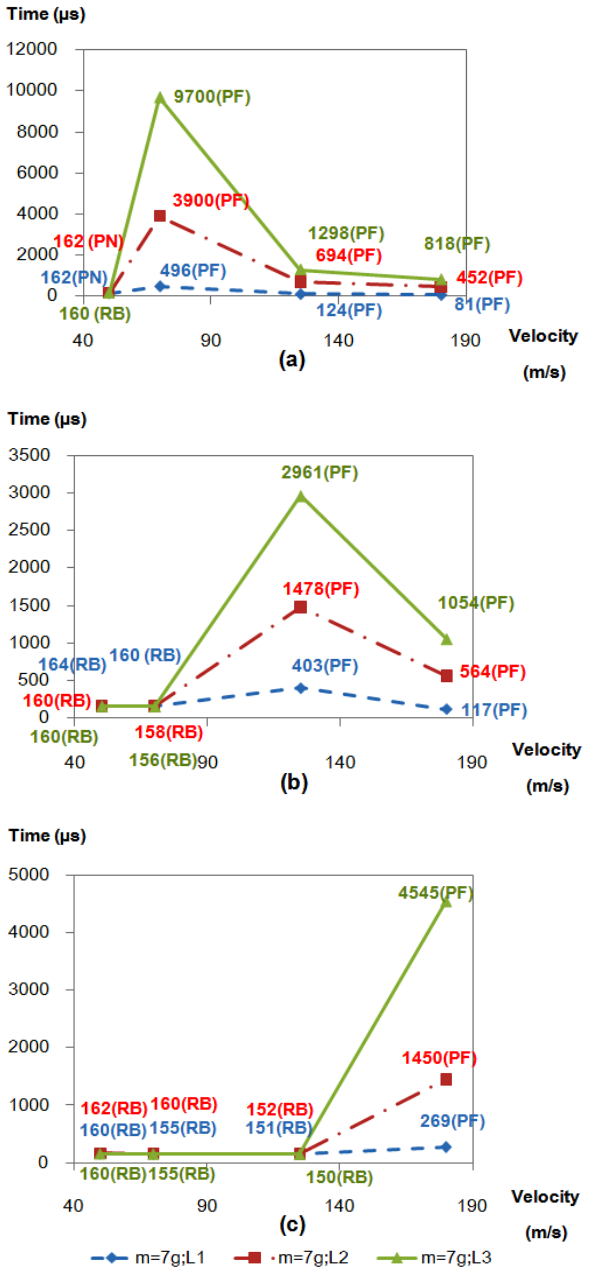

Figure 4. Comparison of total contact time for 7*g* projectiles with different shaft lengths, velocities, and critical failure strains: (a) FS=0.2 (b) FS=0.5 (c) FS=1.

Therefore, changing mass will change the contact time and switching time, leading to a different impact condition and target response. A higher mass will move the impact condition closer to the high mass boundary, as to be expected.

Changing the shaft length only, has no effect unless there is perforation, in which case, effect is very strong.

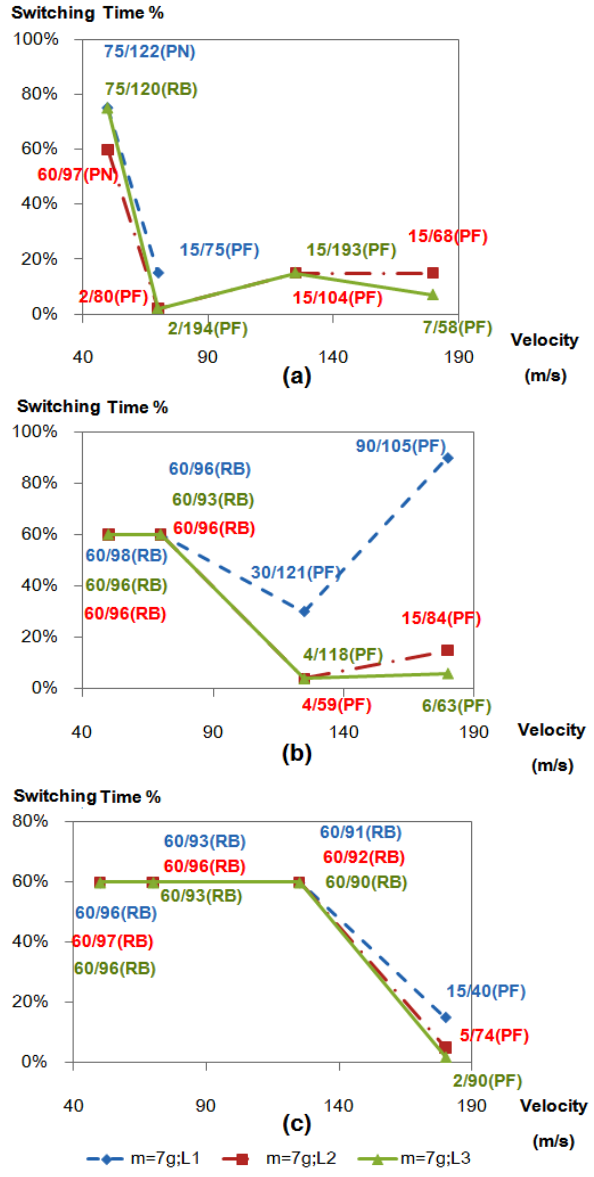

Figure 5. Comparison of switching time for 7*g* projectiles with different shaft lengths, velocities, and critical failure strains: (a) FS=0.2 (b) FS=0.5 (c) FS=1. Showing %/absolute values in microseconds.

3.3 Comments on the damage model

Comparing the simulations with and without the damage model, for rebound cases covering all impact condition regimes, the stress profile shapes and time evolutions show the same characteristics for both models, albeit with some detailed quantitative differences, too numerous to report here. For cases with significant penetration or perforation, the stress profiles show a ripple effect superimposed on the profile shape making it more difficult but still possible to extract other meaningful information such as the switching time. It is believed that the ripple occurs due to the sudden removal of elements and highly localised effects around those elements. It is not easy to know the correct values of FS, or other parameters, even after having checked in the literature [7-11]. FS was chosen as the main parameter to vary to observe its effect on the results. This has been shown in sections 3.1 and 3.2, and is summarised as mainly having the effect of increasing the required velocity (impact energy) to reach the ballistic limit, but with all other characteristic behaviour being unaffected qualitatively, but with related quantitative differences. Clearly, adequate damage models are necessary to generate realistic behaviour when damage is to be expected in the real structures, and is a topic of further development.

4. Conclusion

Increasing projectile shaft length has a clear effect on the resulting impact response for perforation cases, by moving the location in the regime from HV/LM to LV/HM with increasing shaft length. Contact time and % switching time, as defined in the introduction, are good indicators of the resulting regime behaviour, and an increase of shaft length, for all other variables being constant, will increase the contact time and decrease the % switching time. This effect was shown to be sufficient strong, to shift the regime from a full extreme HV/LM condition to nearly a

full extreme LV/HM condition. For rebound cases,

the shaft length has no effect.

5. Acknowledgement

Ms Sarin and Mr Attharat are grateful to the Science and Technology Research Institute (STRI) at KMUTNB for supporting their studies for this work. Mr Attharat is grateful to The Sirindhorn International Thai-German Graduate School of Engineering for funding his attendance and presentation of the paper. Dr Paul Bland is grateful to the U.K. Institution of Mechanical Engineers for funding his attendance and formal representation of the IMechE at the conference. The researchers are grateful to Livermore Software Technology Corporation (LSTC) for the use of their LS-DYNA commercial software.

6. References

[1] Corbett, G. G., Reid, S. R., Johnson, W. (1996). Impact Loading of Plates and Shells by Free-Flying Projectiles: A review, *International Journal of Impact Engineering*, Vol.18, 1996, pp.141-230.

[2] Arias, A., Rodriguez-Martinez, J.A., Rusinek, A. (2008). Numerical simulations of impact behaviour of thin steel plates subjected to cylindrical, conical and hemispherical non-deformable projectiles, *Engineering Fracture Mechanics,* Vol. 75, 2008, pp.1635–1656.

[3] Rusinek, A., Rodriguez-Martinez, J.A., Arias, A., Klepaczko, J.R., and Lopez-Puente, J. (2008). Influence of conical projectile diameter on perpendicular impact of thin steel plate, *Engineering Fracture Mechanics,* Vol. 75, 2008, pp.2946–2967.

[4] Bland, P. W. and Tiranasawasdi, S. (2010). A study on impact mechanics regimes by using stress waves, paper presented in *the 1st TSME International Conference on Mechanical Engineering 2010*, 20-22nd October, Ubon Ratchathani, Thailand.

[5] Tiranasawasdi, S. and Bland, P. W. (2011). A study on impact mechanics regimes by using stress waves, paper presented in the *15th International Annual Symposium on Computational Science and Engineering 2010,* 30th March – 1st April, Bangkok, Thailand.

[6] Bland, P. W. and Tiranasawasdi, S. (2011). A Study of Impact Regime Boundary Transitions, paper presented in *The World Congress on Engineering 2011*, 6-8th July, London, U.K.

[7] Shetty, R., Keni , L., Pai, R. and Kamath, V. (2008). Experimental and analytical study on chip formation mechanism in machining of DRACs, *ARPN Journal of Engineering and Applied Sciences*, vol. 3(5), October 2008, pp.27-32.

[8] Shetty, R., Laxmikant K., Pai, R., and Rao, S. S. (2008). Finite element modelling of stress distribution in the cutting path in machining of discontinuously reinforced aluminium composites: ARPN Journal of Engineering and Applied Sciences.

[9] Avallone, E.A., Baumeister, T., III (1996). Marks' Standard Handbook for Mechanical Engineers, 10th edition, ISBN: 0-07-004997-1, McGraw-Hill, New York.

[10] E.P. Chen (1995). Numerical simulation of penetration of aluminium targets by spherical-nose steel rods, *Theoretical and Applied Fracture Mechanics,* Vol. 22, 1999, pp. 159-164.

[11] MacDonald, B.J. (2002). A computational and experimental analysis of high energy impact to sheet metal aircraft structures, *Journal of Materials Processing Technology*, Vol. 124, 2002, pp.92-98.